Please note that this is an author-produced PDF of an article accepted for publication following peer review. The definitive publisher-authenticated version is available on the publisher Web site

Oecologia
July 2013, Volume 172, Pages 631-643
http://dx.doi.org/10.1007/s00442-012-2527-1
© Springer-Verlag Berlin Heidelberg 2012

Archimer
http://archimer.ifremer.fr

The original publication is available at http://www.springerlink.com

Estimating age at maturation and energy-based life-history traits from individual growth trajectories with nonlinear mixed-effects models

Thomas Brunel[1, *], Bruno Ernande[2], Fabian M. Mollet[1, 3], Adriaan D. Rijnsdorp[1, 4]

[1] Wageningen IMARES, P.O. Box 68, 1970 AB, IJmuiden, The Netherlands
[2] IFREMER, Laboratoire Ressources Halieutiques, 150 quai Gambetta, BP 699, 62321, Boulogne-sur-Mer, France
[3] Blueyou Consulting Ltd., Zentralstrasse 156, 8003, Zürich, Switzerland
[4] Aquaculture and Fisheries Group, Wageningen University, P.O. Box 338, 6700 AH, Wageningen, The Netherlands

*: Corresponding author : Thomas Brunel, email address : thomas.brunel@wur.nl

Abstract:

A new method is presented to estimate individuals' (1) age at maturation, (2) energy acquisition rate, (3) energy expenditure for body maintenance, and (4) reproductive investment, and the multivariate distribution of these traits in a population. The method relies on adjusting a conceptual energy allocation model to individual growth curves using nonlinear mixed-effects modelling. The method's performance was tested using simulated growth curves for a range of life-history types. Individual age at maturation, energy acquisition rate and the sum of maintenance and reproductive investment rates, and their multivariate distribution, were accurately estimated. For the estimation of maintenance and reproductive investment rates separately, biases were observed for life-histories with a large imbalance between these traits. For low reproductive investment rates and high maintenance rates, reproductive investment rate estimates were strongly biased whereas maintenance rate estimates were not, the reverse holding in the opposite situation. The method was applied to individual growth curves back-calculated from otoliths of North Sea plaice (*Pleuronectes platessa*) and from scales of Norwegian spring spawning herring (*Clupea harengus*). For plaice, maturity ogives derived from our individual estimates of age at maturation were almost identical to the maturity ogives based on gonad observation in catch samples. For herring, we observed 51.5 % of agreement between our individual estimates and those directly obtained from scale reading, with a difference lower than 1 year in 97 % of cases. We conclude that the method is a powerful tool to estimate the distribution of correlated life-history traits for any species for which individual growth curves are available.

Keywords: Bioenergetics growth model ; Individual growth trajectory ; Life-history trade-offs ; Energy acquisition ; Maintenance ; Reproductive investment ; Sexual maturation

Introduction

Phenotypic variation in age and size at maturation is of central interest in evolutionary ecology (see reviews in Bernardo (1993), Berrigan and Charnov (1994) and Stearns and Koella (1986)) because of their effects on several fitness components (Stearns and Hoekstra 2005). As for any trait, it may result from genetic variation and/or phenotypic plasticity (Bernardo 1994; Stearns 1984). Genetic variation may occur among populations, among cohorts within populations, and within cohorts (Bernardo 1994; Johnson 2001; Reznick 1990; Stearns 1984). Phenotypic plasticity may occur in response to variability in environmental factors, such as food level (Berrigan and Charnov 1994) and temperature (Atkinson 1994), and to density-dependent processes (Engelhard and Heino 2004), affecting somatic growth and/or the maturation process itself (Bernardo 1993; Dhillon and Fox 2004; Kuparinen et al. 2011; Stearns and Koella 1986). Additionally, age and size at maturation will likely covary with growth rate and reproductive investment, and covariation in these traits might also affect fitness. The analysis of variation in age and size at maturation and covarying life-history traits is hampered by the difficulty to collect data on individual organisms in the wild. Consequently, most studies on variation in growth rate, the onset of sexual maturation and reproductive investment have focused on the population level in the wild or the individual level under experimental conditions.

For many animal taxa, information on individuals' growth history is stored in their calcified structures, such as otoliths and scales in fish, shells in molluscs, endoskeleton in echinoderms, exoskeleton in coral, skeleton in reptiles and amphibians, and teeth in mammals (Campana (2001) and references therein). If the relationship between the size of calcified structures and body size is known, individuals' growth curves can be back-calculated from the distance between successive annual rings in the calcified structures. Estimating individuals' traits from

69 the analysis of back-calculated individual growth curves could then compensate for the lack
70 of direct individual data in wild populations.
71 It has been proposed that individual age and size at maturation can be estimated using
72 segmented regression to detect a “breakpoint” in individual growth trajectories (Baulier and
73 Heino 2008; Rijnsdorp and Storbeck 1995). This breakpoint corresponds to a decrease in
74 somatic growth rate that takes place after maturation as a result of the energy allocation trade-
75 off between reproduction and somatic growth (Roff 1983). Explicit energy allocation models,
76 which derive somatic growth rate as resulting from the balance between energy acquisition
77 and energy expenditures for body maintenance and reproduction, can provide a useful
78 framework to extract more precise and more complete life-history information from back-
79 calculated growth data. Recently, Mollet et al. (2010) fitted an energy allocation-based
80 growth model to individual growth curves back-calculated from fish otoliths in order to
81 estimate age at maturation and the rates of energy acquisition and energy expenditures for
82 maintenance and reproductive investment (hereafter referred to as acquisition rate,
83 maintenance rate and reproductive rate). However, this method, which consists in fitting the
84 model separately for each individual, had some weaknesses. First, the estimates of
85 maintenance rate and reproductive rate were confounded: one was frequently estimated at
86 zero, while the other was estimated as the sum of the two actual rates. The authors overcame
87 this problem either by discarding retrospectively confounded estimates or by assuming that
88 maintenance was constant across individuals. Second, as they are calculated a posteriori from
89 the collection of individual trait estimates, the characteristics (means and (co-)variances) of
90 the traits' distribution in the population are sensitive to any error in individual estimates,
91 including confounding. Third, the method was over-parameterized, 4 parameters being
92 estimated based on 6 to 12 weight-at-age data points depending on individuals.

In the present paper, nonlinear mixed-effects (NLME) modelling is used for fitting an energy allocation model to a set of individual growth curves at once, instead of separately for each individual as done in Mollet et al. (2010). This method first estimates the population level multivariate distribution (means and (co-)variances) of the parameters of interest (assuming they follow a multivariate normal distribution among individuals) and then predicts the individual parameters based on this population level distribution. Hence the population level estimates are not affected by errors in individual estimates and sample properties are naturally extrapolated to the population level. Moreover, the traits are constrained to be normally distributed. Bimodality in the distribution of maintenance and reproductive rates due to confounding as observed in Mollet et al. (2010) is hence avoided. Finally, the NLME framework relies on a likelihood approach which offers the possibility to obtain confidence intervals for the trait means and (co-)variances and to draw statistical inferences (e.g. testing for differences in parameter means between cohorts) , which was not possible with Mollet et al.'s method.

In order to evaluate its performance for different types of life histories, the method is first applied to simulated datasets generated from varying combinations of life-history parameters. Performance is assessed by the accuracy of the estimates of individual parameters and their population distribution characteristics. In a second step, the method is applied to real back-calculated growth curves of Norwegian spring spawning herring (*Clupea harengus*) and North Sea plaice (*Pleuronectes platessa*) (hereafter NSSH and NSP, respectively). The resulting estimates of individual age at maturation and the corresponding population distribution are compared to independent estimates of maturation for each population, i.e. maturity ogives – the proportion of mature individuals at age, also interpreted as the mean probability of being mature at age – for NSP and individuals' age at first spawning estimated by scale reading for NSSH.

Material and methods

Traits estimation procedure

Energy allocation-based growth model

Energy allocation models are based on fundamental biological processes: somatic growth rate is determined by the balance between the acquisition of energy and its utilization for body maintenance and, after maturation, for reproduction. The energy allocation model corresponding to this process of somatic growth is expressed for juveniles and adults as (Ricklefs 2003) :

$$dm/dt = \begin{cases} am^{\alpha} - bm^{\beta} & \text{for } t \le t_{\text{mat}} \\ am^{\alpha} - bm^{\beta} - cm^{\gamma} & \text{for } t > t_{\text{mat}} \end{cases} \quad (1)$$

where m is body mass, t is time, t_{mat} is age at maturation and the coefficients a, b and c are the size-specific rates of energy acquisition, and energy use for body maintenance reproduction, respectively.

For the purpose of illustration, we follow metabolic theory of ecology (West et al. 2001) in choosing $\alpha = 3/4$ and $\beta = \gamma = 1$ (see Electronic Supplementary Material S1). Body mass as a function of time is then given for juveniles $m_J(t)$ and adults $m_A(t)$ by

$$\begin{aligned} m_J(t) &= \left(\frac{a}{b} - \left(\frac{a}{b} - m_0^{\frac{1}{4}} \right) \mathrm{e}^{-\frac{b}{4}t} \right)^4 && \text{for } t \le t_{\text{mat}} \\ m_A(t) &= \left(\frac{a}{b+c} - \left(\frac{a}{b+c} - m_{\text{mat}}^{\frac{1}{4}} \right) \mathrm{e}^{-\frac{b+c}{4}(t-t_{\text{mat}})} \right)^4 && \text{for } t > t_{\text{mat}} \end{aligned} \quad (2)$$

where m_0 is body mass at birth and $m_{\text{mat}} = m_J(t_{\text{mat}})$ is body mass at maturation. Both juvenile and adult growth curves are sigmoid, with asymptotic body mass $m_{\infty J} = (a/b)^4$ and $m_{\infty A} = (a/(b+c))^4$, respectively. After birth, an individual first follows the juveniles curve. It switches to the adult curve at maturation (Fig. 1), after which an additional energy expenditure for reproduction applies. The Heaviside step function, $H(\cdot)$ ($H(x) = 0$ for $x < 0$ and $H(x) = 1$ for $x \geq 0$) is used to combine juvenile and adult growth in a single function for lifetime growth :

$$m(t) = (1 - H(t - t_{\text{mat}}))m_J(t) + H(t - t_{\text{mat}})m_A(t). \quad (3)$$

Statistical model

In order to estimate age at maturation and size-specific acquisition, maintenance and reproductive rates, the energy allocation model $m(t)$ was fitted to cohort-wise sets of individual growth curves using NLME modelling. NLME models are commonly used to fit nonlinear parametric functions to longitudinal data, i.e. repeated measures over time on the same subjects similar to the weight data describing individual growth curves here (Pinheiro and Bates 2000). NLME models primarily estimate the distribution of the parameters in the population - mean values and (co-)variances - and treat each individual as a sample from this distribution. In practice, NLME model represent each individual parameter as the sum of a fixed effect – the population mean of the parameter – and a random effect – the individual parameter's deviation from the mean. The random effects of the different parameters are constrained to follow a multivariate normal distribution centred on 0. The algorithm first estimates the population level distribution characteristics (parameters' means, i.e. fixed effects, and (co-)variances) and predicts the individual parameters (random effects)

afterwards, based on this distribution (but for the sake of simplicity, we will refer to individual values as "estimates").

NLME models were fitted using the nlme package (Pinheiro et al. 2007) of the statistical software R (R Development Core Team 2006). Because of convergence problems when estimating more than 4 parameters, only age at maturation and the 3 size-specific energy rates were estimated, while we set initial body mass to a fixed value equal to its population average.). Confidence intervals of parameter estimates were produced by bootstrapping (1000 replicates) for NSP only as combining NLME and bootstrapping is computationally very intensive. For further details on NLME models and on the fitting procedure used, the reader can refer to Electronic Supplementary Material S2.

Data simulation

The method's performance was evaluated using simulated growth curves datasets representing various life-history types. The 5 free parameters of the energy allocation model (eq. 2) have the dimensions of mass (m_0), time (t_{mat}), time^{-1} (b and c) and mass$^{1/4}$×time^{-1} (a). These parameters can be combined into 3 dimensionless parameters:

$$q = \frac{c}{b+c} = 1 - \frac{b}{b+c}, \qquad \tau_{\mathrm{mat}} = t_{\mathrm{mat}}\left(b+c\right) \qquad \text{and } \nu_0 = m_0\left(\frac{b+c}{a}\right)^4 = \frac{m_0}{m_{\infty A}} \tag{6}$$

so that by varying only q, τ_{mat}, and ν_0 or, equivalently, by setting $1/(b+c)$ and $a/(b+c)$ constant (which amounts to fix the sum $b+c$ and a) while varying c, t_{mat} and m_0, the full range of the model's parameter space can be investigated.

Several datasets of individual growth curves were simulated for different types of life-history strategies by varying mean relative reproductive investment ($\bar{q}$ taking values in $\{1/5;1/3;1/2;2/3;4/5\}$), mean age at maturation ($\bar{t}_{\mathrm{mat}}$ varying between 4 and 8 years in

steps of 1 year) and initial body mass m_0 (taking values in $\{0.5\times10^{-4}\ ;10^{-4}\ ;1.5\times10^{-4}\}$(kg)), while keeping mean size-specific acquisition rate $\bar{a}$ and the sum of mean size-specific maintenance and reproductive rates $\bar{b}+\bar{c}$ constant.

For each dataset corresponding to a given combination $\{\bar{q},\bar{t}_{mat,m_0}\}$, 250 individual growth curves were then generated according to the growth model (3) by sampling randomly individual parameters $\{a_i,b_i,c_i,t_{mat,i}\}$ in a multivariate normal distribution with parameter mean values $\{\bar{a},\bar{b},\bar{c},\bar{t}_{mat}\}$ set as described above and a constant covariance matrix $\mathbf{\Sigma}^2$. The number of years of the simulated growth curves was also sampled randomly in an uniform distribution U(8,18) with the constraint that all individuals should have matured at least one year before they die. Four combinations of $\bar{q}$ and $\bar{t}_{\text{mat}}$, resulting in a maturation body mass higher than asymptotic adult body mass, were discarded from the analysis.

In order to generate realistic growth curves, the fixed parameters ($\bar{a}$, $\bar{b}+\bar{c}$, and $\mathbf{\Sigma}^2$) were given the values obtained by applying the method to a real dataset, namely the 1960 cohort of NSSH (see below for details and values). Since $\bar{a}$ and $\bar{b}+\bar{c}$ were fixed, mean asymptotic body mass $\bar{m}_{\infty A}$ was constant across simulated datasets, but the mean growth curve shape changed according to the mean relative investment to reproduction $\bar{q}$ and the mean age at maturation $\bar{t}_{\text{mat}}$ (Fig. 1).

The energy based growth model (3) was then fitted to each dataset, and the ability of the method to accurately estimate the parameters was assessed by the following measures (where ^ denotes estimate):

- relative error $E_{\bar{x}}=\left(\hat{\bar{x}}-\bar{x}\right)/\bar{x}$ and $E_{\sigma_x}=\left(\hat{\sigma}_x-\sigma_x\right)/\sigma_x$ measuring the bias on estimates of mean $\bar{x}$ and standard deviation σ_x of any parameter.

- absolute error $E_{\rho(x,y)} = \hat{\rho}(x,y) - \rho(x,y)$ for the bias on correlation $\rho(x,y)$ between any pair of parameters (x,y),
- mean of the absolute values of individual relative errors $E_x = (\sum_i |\hat{x}_i - x_i| / x_i)/n$ as a measure of the imprecision of the individual estimates for any parameter x (n being the number of individuals)

Real datasets

The method was applied to individual growth data for NSP (from IMARES, IJmuiden, Netherlands) and NSSH (from Institute of Marine Research, Bergen, Norway). For NSP, length-at-age data were back-calculated from otoliths sampled from the Dutch commercial catches between 1933 and 1999. Length l was converted into body mass m using the allometric relationship $m = \delta l^{\theta}$ with $\delta = 10^{-5}$ kg.cm^{-1} and $\theta = 3$ (Rijnsdorp and Storbeck 1995). For NSSH, length-at-age data were back-calculated from scales sampled from commercial catches and scientific surveys between 1935 and 1973. These were transformed into body mass using a similar allometric relationship with $\delta = 2.32 \times 10^{-5}$ kg.cm^{-1} and $\theta = 2.81$ (Jennings and Beverton 1991). A description of the data collection and back-calculation methods including the respective validations can be found in Rijnsdorp et al. (1990) for NSP, and Engelhard et al. (2003) for NSSH. For each stock, two cohorts, one characterized by early maturation and one by late maturation, were chosen to test our method. Only mature females older than 6 years were considered in this study.

To assess the validity of our method, estimates (named thereafter growth-based estimates) of age at maturation were compared to independent estimates. For NSP, no independent individual estimate of age at maturation was available and the validity of the method was assessed at the population level. The observed maturity ogive $o_o(t)$ – the proportion of

mature individuals at age t – was calculated for each cohort from commercial catches sampling where individual maturity status was determined by visual inspection of the gonad (from Rijnsdorp and Storbeck (1995)). The growth-based individual estimates of age at maturation $\hat{t}_{\text{mat},i}$ were used to calculate the probability of maturing at a given age t conditional on being still immature at age $t-1$, $p(t)$ (i.e. $p(t) =$ number of individuals with $t-1 < \hat{t}_{\text{mat},i} < t$ divided by the number of individuals with $\hat{t}_{\text{mat},i} > t-1$). Under the assumption that mortality rate does not differ between immature and mature individuals; a growth-based estimate of the maturity ogive, $o_g(t)$, was then derived from the probability of maturing at a given age (see Kuparinen et al. (2008) for details) :

$$o_g(t) = \sum_{\hat{t}_{\text{mat},i}=1}^{t-1} \left[\left(\prod_{t'=0}^{\hat{t}_{\text{mat},i}-1} (1 - p(t')) \right) p(\hat{t}_{\text{mat},i}) \right] \text{ for } t > 1 \quad (7)$$

A logistic model was then fitted to the maturity ogives estimated from the sampling of commercial catches and from the growth-based $\hat{t}_{\text{mat}}$:

$$o(t) = {}^{1}/_{1 + e^{-(\omega + kt)}} \quad (8)$$

The age at which 50% of the individuals are mature $A_{50} = -\omega/k$ and slope k of the ogive were used to compare the maturity ogives.

For NSSH, the comparison was carried out at the individual level. Winter and summer growth layers on NSSH scales differ between spawning and non-spawning years (Runnström 1936). A direct estimate of age at first spawning was hence 'read' on each individual scale. Since an individual maturing in its Y^{th} year (Y being an integer) will reproduce for the first time at age Y+1, the growth-based estimates of individuals' age at maturation, $\hat{t}_{\text{mat,i}}$, were rounded to the

next integer to be converted into age at first spawning, $\hat{T}_{\text{mat,i}}$. Growth-based individual estimates $\hat{T}_{\text{mat,i}}$ were then directly compared with scale-based estimates $T_{\text{mat,i}}$.

Results

Simulated data

Results for the datasets with $m_0 = 10^{-4}$ kg are presented first in order to investigate the influence of $\bar{q}$ and $\bar{t}_{mat}$ on the method's performance. Results for varying values of m_0 are presented at the end of this section.

Estimation of the multivariate distribution of the life history parameters in the population

The parameter means $\{\bar{a}, \bar{b}, \bar{c}, \bar{t}_{mat}\}$ were generally accurately estimated (Fig. 2). Bias for $\bar{a}$ and $\bar{t}_{\text{mat}}$ was generally very low with $E_{\bar{a}}$ and $E_{\bar{t}_{mat}}$ less than 0.01 (but $E_{\bar{a}} = 0.06$ for $\bar{q} = 4/5$ and $\bar{t}_{mat} = 4$yr, and $E_{\bar{t}_{mat}} = -0.09$ for $\bar{q} = 1/5$ and $\bar{t}_{mat} = 4$yr).

Bias in estimates of $\bar{b}$ and $\bar{c}$ was moderate with opposite patterns. $\bar{b}$ was well estimated for low $\bar{q}$ and early maturation ($|E_{\bar{b}}| \leq 0.09$ for $\bar{q} \leq 1/2$ and $\bar{t}_{mat} \leq 5$yr), but under increased $\bar{q}$, bias became larger (up to $E_{\bar{b}} = -0.21$). In contrast, $E_{\bar{c}}$ was generally positive and lower than 0.10 for moderate to high $\bar{q}$ and late maturation. Bias increased when $\bar{q}$ was low and maturation relatively early (up to $E_{\bar{c}} = 0.19$ for $\bar{q} = 1/5$ and $\bar{t}_{mat} = 6$yr). The sum $\bar{b} + \bar{c}$, however, was almost always well estimated ($|E_{\overline{b+c}}| \leq 0.05$), suggesting that errors in $\bar{b}$ and $\bar{c}$ were compensating each other.

Standard deviations of the life history parameters were generally overestimated with bias larger than for their means (Fig. 3; notice the difference of scale between this figure and Fig. 2). Bias for $\sigma_{t_{mat}}$ was low to moderate ($E_{\sigma_{t_{mat}}}$ varying between -0.07 and +0.14). Bias for

σ_a was also moderate (E_{σ_a} being almost always positive and below 0.15) for low $\bar{q}$ and early mean maturation ($\bar{q} \leq 1/2$ and $\bar{t}_{\text{mat}} \leq 6yr$), but increased for higher $\bar{q}$ and later maturation with E_{σ_a} between 0.25 and 0.30. Again, patterns of bias for σ_b and σ_c were opposite. For $\bar{q} \leq 1/3$, the bias for σ_b was moderate ($|E_{\sigma_b}| \leq 0.17$). However, for higher $\bar{q}$, the bias increased strongly ($-0.30 \leq E_{\sigma_b} \leq 0.42$ for $\bar{q}$ in $\{1/2\,;\,2/3\}$ and increasing up to 0.70 for $\bar{q} = 4/5$). Bias on σ_c was generally moderate to low ($|E_{\sigma_c}| \leq 0.10$), except for low $\bar{q}$ and early maturation ($E_{\sigma_c} = 0.40$ for $\bar{q} = 1/5$ and $\bar{t}_{mat} = 4$yr).

The bias in the estimation of correlations between pairs of life history parameters varied according to the parameters involved (Fig. 3; notice that bias on correlation are expressed as absolute errors). Correlations $\rho(a,c)$, $\rho(a,t_{\text{mat}})$, and $\rho(c,t_{\text{mat}})$ were accurately estimated (errors between -0.15 and +0.15) except under low $\bar{q}$ ($\bar{q} = 1/5$) and/or early maturation ($\bar{t}_{mat} = 4$yr), when correlation estimates were clearly inaccurate (e.g. $E_{\rho(a,c)} = 0.61$). For correlations involving the size-specific maintenance rate *b*, the bias was stronger with errors varying generally between -0.3 and +0.3 with no clear pattern, but rising up to $E_{\rho(b,t_{mat})} = 0.48$ and decreasing to $E_{\rho(a,b)} = -0.81$ when $\bar{q}$ was high and mean age at maturation was low ($\bar{q} = 4/5$ and $\bar{t}_{mat} = 4$yr).

Estimates of the individual life-history parameters

The accuracy of the individual trait estimates varied across parameters, and, for a given parameter, varied according to the values of $\bar{q}$ and mean age at maturation $\bar{t}_{\text{mat}}$ (Fig. 4). The patterns observed were generally the same as for the bias on the mean parameters. Individual size-specific acquisition rate a_i was well estimated, with $E_a \leq 0.05$ for all datasets. Estimates of individual age at maturation $\hat{t}_{\text{mat},i}$ were also very accurate ($E_{t_{\text{mat}}} < 0.025$), although the error increased moderately (up to $E_{t_{mat}} = 0.10$) for low mean age at maturation

($\bar{t}_{mat} = 4$yr) and low $\bar{q}$. In most cases, the method failed to estimate correctly individual size-specific maintenance and reproductive rates. The error for b_i was on average higher than for c_i. In addition, the errors E_b and E_c varied in opposite directions with $\bar{q}$. b_i was accurately estimated for low $\bar{q}$ ($E_b < 0.08$ for $\bar{q} = 1/5$), but errors were higher for higher $\bar{q}$, especially at low mean age at maturation (up to $E_b = 0.40$ for $\bar{q} = 4/5$ and $\bar{t}_{mat} = 4$yr). In contrast, E_c was low for high $\bar{q}$ ($E_c < 0.08$ for $\bar{q} \geq 2/3$, except for $\bar{q} = 4/5$ and $t_{\text{mat}} = 4yr$ where $E_c = 0.13$) but increased markedly for low $\bar{q}$ (E_c between 0.11 and 0.19 for $\bar{q} \leq 1/3$). However, E_b and E_c compensated so that the sum E_{b+c} was accurately estimated in all cases.

Sensitivity to initial body mass

The method's performance was almost insensitive to the value of initial body mass m_0. The accuracy of the estimates of parameter means, standard deviations and correlations was similar whatever the value of m_0 (results not shown). Furthermore, the level of error for individual parameter estimates was hardly affected by the value of m_0 (Table 1).

Real data

The energy allocation-based growth model fitted very well to the individual growth curves in the four datasets considered ($R^2 > 0.98$ in all cases).

For both species, estimates of the mean age at maturity $\hat{\bar{t}}_{mat}$ were different between cohorts, although the confidence intervals largely overlapped for NSP (Table 2 and 3). Estimates of mean size-specific energy allocation rates $\hat{\bar{a}}$, $\hat{\bar{b}}$ and $\hat{\bar{c}}$ varied between the cohorts (except for $\hat{\bar{a}}$ for NSSH). Furthermore, mean size-specific acquisition rate $\hat{\bar{a}}$ was substantially higher in NSP than in NSSH, whereas mean size-specific maintenance $\hat{\bar{b}}$ and reproductive $\hat{\bar{c}}$ rates were relatively similar for the two species. The estimated mean relative reproductive

investment $\hat{\bar{q}} = \hat{\bar{c}}/(\hat{\bar{b}} + \hat{\bar{c}})$ differed between cohorts for NSP (0.24 and 0.63 for the 1963 and 1969 cohorts respectively) but less for NSSH (0.44 and 0.53 for the 1933 and 1960 cohorts respectively).

The correlation structure between parameters was similar both between cohorts and between species (Table 2 and 3). The correlation $\hat{\rho}(a, b)$ was always high and positive and the correlation $\hat{\rho}(a, t_{mat})$was always negative (although the confidence interval for the 1963 cohort for NSP included 0). The correlation $\hat{\rho}(c, t_{mat})$ was always high and negative. The correlations $\hat{\rho}(a, c)$ and $\hat{\rho}(b, t_{mat})$ were almost always weak (expect for the 1960 cohort in NSSH). While the correlation $\hat{\rho}(b, c)$ was low for NSSH, high negative values were observed for NSP.

The NLME framework allows performing statistical tests on population level characteristics (parameters' means and (co-)variances), which is illustrated here on NSP (Table 2). For the two year-classes of NSP, likelihood ratio tests indicated that the 4 life-history parameters varied significantly among individuals (significant variances, $p<0.001$) and were significantly correlated (significant covariances, $p<0.001$). Furthermore, F tests and a likelihood ratio tests respectively showed that the mean values (fixed effect) of the four traits and the covariance matrix of the random effects differed significantly between the 1963 and 1969 cohorts ($p<0.001$ in all cases).

For both cohorts of NSP, the maturity ogives reconstructed from gonad inspection in commercial samples and from the growth-based estimates were very similar (Fig. 5) with very close A_{50} values ($A_{50,o,1963} = A_{50,g,1963} = 4.27yr$ and $A_{50,o,1969} = 3.21$yr vs. $A_{50,g,1969} = 3.00$yr where subscripts o refers to maturity status observations and g to growth-based) and rather similar slopes ($k_{o,1963} = 1.53\ vs.\ k_{g,1963} = 1.11$ and $k_{o,1969} = k_{g,1969} = 1.71$). For NSSH, the percentage of agreement between the growth-based estimates and the scale-based estimates of individual age at first reproduction were of 61 % and 46 % for cohort 1933 and

1960, respectively (Table 4). For both cohorts, the agreement was slightly lower for individuals with early maturation (for scale-based age at maturation of 5 years, only 46% and 30% of agreement) whereas it was much higher for individuals maturing older. For most individuals, the difference between growth-based estimates and scale-based estimates was less than or equal to one year (94% and 98% for cohort 1933 and 1960, respectively).

Discussion

Accuracy of estimates of individual life-history parameters and their population distribution

Our study on simulated data indicates that the accuracy of the estimates varies across parameters and according to the species' life-history type. For age at maturation, size-specific energy acquisition rate, and the sum of size-specific maintenance and reproductive rates, population distribution and individual parameters are accurately estimated for all life-history types. In contrast, while they are moderately accurate for the most common life-history strategies, the estimates of size-specific maintenance and reproductive investment rates are clearly poor for extreme life-history types. Size-specific reproductive investment rate is poorly estimated for low reproductive investment because this results in a weaker decrease in somatic growth after maturation (Fig. 1). On the opposite, a high reproductive investment leads to biased estimates of size-specific maintenance rate. This is due to the symmetric roles of these two energy rates in determining asymptotic body mass, $m_{\infty A} = (a/(b+c))^4$. Asymptotic body mass and the speed to reach it are estimated accurately, whereas the method fails in distinguishing maintenance from reproduction when imbalance between the two parameters is large. The discrimination ability of the method could be improved by integrating data on reproductive investment. Annual reproductive investment can be assessed

363 from biological data as the sum of the gonads' energy content before spawning (often
364 measured by proxies, such as the gonado-somatic index) and, if relevant, the energy spent for
365 spawning migration (see Mollet et al. (2010)) for an example on NSP). The energy allocation
366 model could then be fitted to growth and reproductive investment data together by modelling
367 annual reproductive investment as the energy accumulated in the reproductive compartment
368 during one year. However, reproductive investment is generally difficult to measure,
369 especially energy expenditure for spawning migration. Finally, the method was insensitive to
370 the initial body mass value. This supports the choice made here to reduce the number of
371 parameters estimated by assuming a constant initial body mass.
372 The distribution of age at maturation for both cohorts of NSP was accurately estimated by the
373 method, as shown by the high agreement between growth-based and gonad observation based
374 the maturity ogives. For NSSH, estimates of age at first spawning (calculated from the
375 growth-based individual estimates of age at maturation) agreed reasonably well with the scale
376 reading-based ones. The differences between growth-based and scale reading estimates of age
377 at first spawning do not necessarily mean that the growth-based estimates are erroneous, and
378 could also be attributed to errors in scale reading. It is believed that scale estimates are of
379 good quality, but the scale reading method has not been validated, and the level of error or
380 bias is unknown (Baulier and Heino, 2008). Scale readers estimate age at maturation based on
381 the distinction between relatively wide 'coastal' and 'oceanic' rings, corresponding to the
382 immature stage, and narrow 'spawning' rings, corresponding to years after first spawning
383 (Runnström 1936). In some cases, this distinction may be problematic, especially when the
384 last oceanic ring corresponding to the maturation year has an intermediate width (Engelhard
385 et al. 2003).

Variation in North sea plaice and Norwegian spring spawning herring life-history parameters

The application of the method to NSP and NSSH data revealed differences in the life-history parameters between cohorts, in both species. Such variation may result from phenotypic plasticity in response to environmental variations. For instance, energy acquisition is related to food availability (e.g. Kooijman (2000)) which, in turn, depends on the productivity of prey species and on the intensity of the competition for resources. Any variation in environmental factors (e.g. temperature, eutrophication) affecting food productivity, or any change in the abundance of the species competing for the same food, will therefore influence the energy acquisition rate. Changes in temperature also affect the metabolism of individuals, thereby causing variation in size-specific maintenance rate *b* (Atkinson, 1994).

Temporal variation in energy-based life history traits will result in different growth patterns and, as maturation is closely correlated with growth (Stearns and Koella, 1986), in different timing for the onset of maturation. For instance, the very large 1963 cohort for grew slowly and matured late, probably due to an increased density-dependent competition for food (Rijnsdorp and Van Leeuwen 1992), which also reflects in the lower size-specific acquisition rate for this cohort. Density-dependence may also explain the earlier maturation of the 1960 cohort in NSSH, which grew up in an environment with fewer conspecifics than the 1933 one. The two cohorts being almost 3 decades apart, evolutionary changes might also have happened in response to natural or human-induced selection or both (Engelhard and Heino 2004). The higher reproductive investment in the 1960 cohort than in the 1933 one is in agreement with the expectations from fisheries-induced evolution theory.

Applying our method to the whole dataset of back-calculated growth curves for the two species would provide historical time-series of life-history traits. The analysis of the

410 covariation between these time-series and explanatory variables could help to disentangle the
411 respective influence of evolution and phenotypic plasticity.

412 ***Comparison with other estimation methods***

413 The first method proposed for estimating age at maturation from individual growth curves
414 was a piecewise linear regression of individual annual body mass increments against body
415 mass to detect the 'breakpoint' corresponding to the decrease in somatic growth occurring
416 after maturation (Rijndorp and Storbeck, 1995). This method was applied recently to Irish Sea
417 plaice (Scott and Heikkonen 2012) and to NSSH (Baulier and Heino 2008). In NSSH a 47.6%
418 agreement between the 'breakpoint' estimates of age at maturation and those read from scale
419 marks was obtained, with the highest disagreement found for late maturing individuals.
420 Larger error for late maturing individuals may come from the fact that, under the common
421 assumption that maintenance energy scales with a greater power of body mass than energy
422 acquisition ($\beta > \alpha$), maintenance rate increases with body mass faster than acquisition rate,
423 so that growth rate decreases when body mass exceeds a threshold value $m_{\mathrm{th}} = (b\beta/a\alpha)^{(\beta-\alpha)}$
424 (from equation (1) when the derivative of growth rate $\partial m_J / \partial t$ for m is set to 0). If an
425 immature individual reaches m_{th} , the piecewise regression will detect a breakpoint at the age
426 corresponding to m_{th}, which is earlier than maturation. Our method does not suffer from this
427 problem because the underlying energy allocation model integrates explicitly the faster
428 increase of maintenance rate with body mass. In another study, age at maturation in NSSH
429 was estimated from the width of the annual growth layers in scales by discriminant analysis
430 and artificial neural networks resulting in 67% of agreement with the estimates of age at
431 maturation read in scale marks (Engelhard et al. 2003). However, these methods require to be
432 calibrated using a training dataset consisting of individuals for which the age at maturation is

433 known. In contrast, the method presented here does not require any *a priori* knowledge and
434 therefore can be applied to any species for which individual growth trajectories are available.
435 The methods presented in this study and in Mollet et al. (2010) are the first to estimate
436 individual life-history traits simultaneously from individual growth data. These methods
437 accurately estimate the distribution of age at maturation in the population as shown by the
438 comparison of the maturity ogives for NSP in the present study and with maturation reaction
439 norms in Mollet et al. (2010). In the present study, we provide a second validation of the
440 method on real dataset allowing to test the accuracy of the individual age at maturation
441 estimates, by comparing the output of the NLME with estimates read directly from maturation
442 marks on scales for NSSH.
443 The NLME method developed in this paper results in substantial improvements compared to
444 the individual optimisation fit performed in Mollet et al (2010). First, the NLME method
445 reduces the confounding problem between size-specific maintenance and reproductive rates to
446 species with extreme life-history strategies only (see above). The bimodality problem
447 observed in Mollet et al. as a result of confounding is avoided here because the individual
448 parameters are forced to follow a (multivariate) normal distribution. Second, in Mollet et al,
449 the characteristic of the traits distribution in the population, calculated from the individual
450 estimates, are affected by any source of error in the individual estimates (including the
451 bimodality problem, unless a fixed size-specific maintenance rate was assumed). Within the
452 NLME framework, population-level parameters are directly estimated as the fixed effects
453 (mean traits) and (co-)variances between traits, and are independent of the individual
454 estimates of the traits that are calculated *a posteriori*. Third, the individual optimisation
455 method is over-parameterized (4 parameters are estimated for each individual from only 6 to
456 12 growth data points) whereas the NLME method reduces the number of parameters to be
457 estimated to 14 (4 fixed effects and 10 (co-)variances) for the whole dataset thus leading to

458 more stable estimates. Finally, the NLME framework is based on a likelihood approach that
459 allows to draw statistical inferences such as testing for differences in the multivariate
460 distribution (means and (co-)variances) of the life-history parameters between distinct groups
461 of individuals (e.g. cohorts) or for the dependence of the population mean traits on
462 explanatory variables (e.g. by including temperature as a covariate; not implemented here).
463 Hence, the NLME method appears more appropriate to characterise the multivariate
464 distribution of life-history parameters in a population and is particularly suitable for
465 evolutionary ecologists who are often more interested in the distribution of traits in a
466 population than in any particular individual values. Although our method may not necessarily
467 provide unbiased estimates of the life history parameters, it provides a consistent
468 interpretation of the data which in many applications matters more.

469 ***Limitations and applicability***

470 From a practical point of view, the NLME algorithm requires a sufficiently large sample of
471 individuals (e.g., $n \geq 30$) as well as a sufficiently large number of age-size records per
472 individual, notably during the adult stage, to ensure proper estimation of the decrease in
473 growth rate due to reproductive investment. It may occur that, for a given set of starting
474 values, convergence cannot be reached by the estimation algorithm. It is therefore advised to
475 try various combinations of initial values and test the solutions for their respective goodness
476 of fit and convergence.
477 Given that the performance depends on the life-history strategy, we also recommend, when
478 applying the method to a new species, to evaluate its performance using simulated data in a
479 similar setup as the one presented here.
480 We would also like to remind the reader that the values of the traits estimated by the method
481 are conditional to the value of the scaling exponents of energy rates with body mass. As long
482 as $\alpha < \beta$ and $\alpha < \gamma$, using different exponent value would rescale the estimates of the size-

specific energy rates, but would not affect estimates of age at maturation. The method would still provide accurate estimates of age at maturation and remain suitable to study the relative differences or changes in the mean and (co-)variances of the other traits.

A potential limitation of our method is that the energy allocation model does not include energy reserves. For NSP for instance, first-time spawners can use all surplus energy for somatic growth because they already have the high energy reserves required for spawning. In contrast, repeat spawners need to rebuild their energy reserves (that are depleted due to spawning the previous year) for the next spawning event before using energy for somatic growth (Rijnsdorp 1990). Hence, first time and repeat spawners start their respective year of reproduction in different energetic conditions, and the growth cost of reproduction may therefore become manifest only from the second spawning year onwards. This could result in an overestimation of age at maturation by our method. Nevertheless, the strong similarity between the growth- and gonad-based maturity ogives observed for NSP suggests that our simplification of energy dynamics has little implications for our primary purpose to estimate age at maturation.

Another implicit simplification of the energy allocation model is that the rates of energy acquisition and expenditure are only determined by body mass and not affected by environmental variation, for instance in temperature or food availability, despite substantial empirical evidence (e.g. Brander (1995) or Mollmann et al. (2005)). The effect of neglecting temporal variability in size-specific energy rates might reduce the precision of the estimates and result, if temporal variability is strong, in estimation biases (Mollet et al. 2010). However, the environmental variability levels for which these effects are substantial are unlikely to be common in nature (Mollet et al. 2010).

Although individual-level estimates of the parameters may be partly biased in some circumstances, the relatively good accuracy of the estimates of their population means,

standard deviations and correlations provides potential for a wide range of applications. Firstly, maturity ogives can be calculated from the estimated mean and variance of age at maturation in each cohort. In the context of fish stock assessment for instance, this provides an alternative to the traditional estimation of maturity ogives based on the determination of fish maturity stage by visual inspection of the gonads, which is potentially affected by various sources of errors (see also Scott and Heikkonen (2012)). Moreover, for many fish stocks, maturity data are too scarce to estimate a maturity ogive for each cohort, so that temporal variations in maturity cannot be accounted for. Coupled with automated otolith analyses (Fablet and Le Josse 2004), our method would complement a powerful toolbox to analyse large collections of otoliths and provide historical time series of maturity ogives improving the reconstruction of historical spawning stock biomass time series. The application is not restricted to fish, but can be applied to any other taxa with calcified structures allowing the back-calculation of individual growth trajectories. Our method also provides the potential to study life-history strategies, in particular the phenotypic correlations between life-history traits that can help improve our understanding of life-history trade-offs and intraspecific variation in life-history.

Acknowledgements

The authors would like to thank the Institute of Marine Research (Bergen, Norway) for providing the data on NSSH. We are also grateful to Mikko Heino and two anonymous reviewers for their critical comments which greatly helped in improving the manuscript. This study was supported by the European research training network FishACE and the strategic research program "Sustainable spatial development of ecosystems, landscapes, seas and regions" funded by the Dutch Ministry of Agriculture, Nature Conservation and Food Quality.

References

Atkinson D (1994) Temperature and organism size - a biological law for ectotherms. Advances in Ecological Research 25:1-58

Baulier L, Heino M (2008) Norwegian spring-spawning herring as the test case of piecewise linear regression method for detecting maturation from growth patterns. Journal of Fish Biology 73:2452–2467

Bernardo J (1993) Determinants of maturation in animals. Trends in Ecology and Evolution 8:166-173

Bernardo J (1994) Experimental analysis of allocation in two divergent, natural salamander populations. American Naturalist 143:14-38

Berrigan D, Charnov EL (1994) Reaction norms for age and size at maturity in response to temperature - a puzzle for life historians. Oikos 70:474-478

Brander KM (1995) The effect of temperature on growth of Atlantic cod (*Gadus morhua L.*). ICES Journal of Marine Science 52:1-10

Campana SE (2001) Accuracy, precision and quality control in age determination, including a review of the use and abuse of age validation methods. Journal of Fish Biology 59:197 - 242

Dhillon RS, Fox MG (2004) Growth-independent effects of temperature on age and size at maturity in Japanese medaka (*Oryzias latipes*). Copeia 2004:37-45

Engelhard GH, Dieckmann U, Godø OR (2003) Age at maturation predicted from routine scale measurements in Norwegian spring-spawning herring (*Clupea harengus*) using discriminant and neural network analyses. ICES Journal of Marine Science 60:304-313

Engelhard GH, Heino M (2004) Maturity changes in Norwegian spring-spawning herring Clupea harengus: compensatory or evolutionary responses? Marine Ecology Progress Series 272:245–256

Fablet R, Le Josse N (2004) Automated fish age estimation from otolith images using statistical learning. Fisheries Research 72:279–290

Jennings S, Beverton RJH (1991) Intraspecific variation in the life history tactics of Atlantic herring (*Clupea harengus* L.) stocks. ICES Journal of Marine Science 48:117-125

Johnson JB (2001) Adaptive life-history evolution in the livebearing fish *Brachyrhaphis rhabdophora*: Genetic basis for parallel divergence in age and size at maturity and a test of predator-induced plasticity. Evolution 55:1486-1491

566 Kooijman SALM (2000) Dynamics enregy and mass budgets in biological systems.
567 Cambridge University Press, Cambridge, UK
568 Kuparinen A, Cano J, Loehr J, Herczeg G, Gonda A, Merila J (2011) Fish age at maturation is
569 influenced by temperature independently of growth. Oecologia Aquatica 167:435-443
570 Kuparinen A, O'Hara RB, Merilä J (2008) The role of growth history in determining the age
571 and size at maturation. Fish and Fisheries 9:201-207
572 Mollet FM, Ernande B, Brunel T, Rijnsdorp AD (2010) Multiple growth-related life history
573 traits estimated simultaneously in individuals. Oikos 119:10-26
574 Mollmann C, Kornilovs G, Fetter M, Koster FW (2005) Climate, zooplankton, and pelagic
575 fish growth in the central Baltic Sea. ICES Journal of Marine Science 62:1270-1280
576 Pinheiro, J. C. and Bates, D. M. (2000). Mixed Effects Models in S and S-Plus. New York:
577 Springer. 528pp.
578 Pinheiro J.C., Bates D.M., DebRoy S, Sarkar D, the R Core team (2007) nlme: Linear and
579 Nonlinear Mixed Effects Models. R package version 3.1-86
580 R Development Core Team (2006) R: A language and environment for statistical computing.
581 R Foundation for Statistical Computing, Vienna, Austria
582 Reznick DN (1990) Plasticity in age and size at maturity in male guppies (*Poecilia reticulata*)
583 - an experimental evaluation of alternative models of development. Journal of
584 Evolutionary Biology 3:185-203
585 Ricklefs RE (2003) Is rate of ontogenetic growth constrained by resource supply or tissue
586 growth potential? A comment on West et *al.'s* model? Functional Ecology 17:384-393
587 Rijnsdorp AD (1990) The mecanism of energy allocation over reproduction and somatic
588 growth in the female North Sea plaice, *Pleuronectes platessa* L. Netherlands journal
589 of Sea Research 25:279-290
590 Rijnsdorp AD, Storbeck F (1995) Determining the onset of sexual maturity from otoliths of
591 indiviual female North Sea plaice, *Pleuronectes platessa* L. In: Secor D, Dean J,
592 Campana S (eds) Recent developments in fish otolith research. University of South
593 Carolina Press, Columbia, pp 581-598
594 Rijnsdorp AD, Van Leeuwen PI (1992) Density dependent and independent changes in
595 somatic growth of female North Sea plaice *Pleuronectes platessa* between 1930 and
596 1985 as revealed by back-calculation of otoliths. Marine Ecology Progress Series
597 88:19-32

598 Rijnsdorp AD, van Leeuwen PI, Visser TAM (1990) On the validity and precision of back-
599 calculation of growth form otoliths of the plaice, *Pleuronectes platessa L*. Fisheries
600 Research 9:97-117
601 Roff DA (1983) An allocation model of growth and reproduction in fish. Canadian Journal of
602 Fisheries and Aquatic Sciences 40:1395-1404
603 Runnström S (1936) A study on the life history and migrations of the Norwegian spring-
604 spawning herring based on the analysis of the winter rings and summer zones of the
605 scales. Fiskeridirektoatets Skrifter, Serie Havundersokelser 5:1-103
606 Scott RD, Heikkonen J (2012) Estimating age at first maturity in fish from change-points in
607 growth rate. Marine Ecology Progress Series 450:147-157
608 Stearns SC (1984) The effects of size and phylogeny on patterns of covariation in the life
609 history traits of lizards and snakes. The American Naturalist 123:56-72
610 Stearns SC, Hoekstra RJ (2005) Evolution. 2nd Ed. Oxford University Press, New York
611 Stearns SC, Koella JC (1986) The evolution of phenotypic plasticity in life-history traits:
612 predictions of reaction norms for age and size at maturity. Evolution 40:893-913
613 West GB, Brown JH, Enquist BJ (2001) A general model for ontogenetic growth. Nature
614 413:628-631
615
616
617

Tables :

Table 1. Influence of initial body mass on the accuracy of the individuals' trait estimates. For each value of m_0, $\overline{E_x}$ is the average of E_x (the error on the individual estimates for each parameter *x*) over the simulated datasets corresponding to all possible combination of $\bar{q}$ and $\bar{t}_{mat}$.

m_0	$\overline{E_a}$	$\overline{E_b}$	$\overline{E_c}$	$\overline{E_{b+c}}$	$\overline{E_{t_{mat}}}$
0.5×10^{-4}kg	0.052	0.213	0.141	0.065	0.027
1×10^{-4}kg	0.047	0.249	0.144	0.059	0.024
1.5×10^{-4}kg	0.056	0.205	0.113	0.070	0.020

Table 2. Estimates of the life-history parameters, their correlation matrix and associated statistical tests for two year-classes of NSP (F.E.: fixed effects, sd(R.E): standard deviation of random effects) and their confidence intervals estimated by bootstrap (numbers in brackets). Units are yr for t_{mat}, yr^{-1} for *b* and *c* and $kg^{1/4}.yr^{-1}$ for *a*. Hypothesis tests are based on F tests for fixed effects and likelihood ratio tests between nested models that asymptotically follow a χ^2 under the null hypothesis for random effects' (co-)variances (Pinheiro and Bates 2000).

	North Sea plaice			
	YC 1963		**YC 1969**	
N	158		109	
Parameter mean and standard deviation estimates				
	F.E	sd(R.E)	F.E	sd(R.E)
a	0.87 (0.83;0.89)	0.16 (0.14;0.18)	0.92 (0.86;0.98)	0.19 (0.16;0.22)
b	0.57 (0.42;0.67)	0.23 (0.16;0.28)	0.30 (0.01;0.45)	0.29 (0.01;0.39)
c	0.18 (0.10;0.29)	0.13 (0.10;0.18)	0.53 (0.33;0.70)	0.25 (0.18;0.32)
t_{mat}	4.76 (3.63;6.12)	1.70 (1.32;2.14)	3.81 (3.35;4.14)	0.99 (0.73;1.41)
Parameter correlation estimates				
	a	*b*	*a*	*b*
b	0.72 (0.36;0.85)		0.67 (0.19;0.82)	
c				

c	0.16 (-0.16;0.59)	-0.53 (-0.64;-0.37)		0.14 (-0.17;0.96)	-0.64 (-0.76;-0.00)	
t_{mat}	-0.40 (-0.72;0.10)	0.25 (-0.18;0.57)	-0.77 (-0.89;-0.51)	-0.65 (-0.93-;-0.38)	0.08 (-0.57;0.47)	-0.80 (-0.92;-0.57)

Statistical tests :

The traits are variable among individuals[1]

$\chi^2_4 = 2150$,p<0.001 $\chi^2_4 = 360$, p<0.001

The traits are correlated[2] :

$\chi^2_6 = 442$,p<0.001 $\chi^2_6 = 418$, p<0.001

Difference in traits' mean values between the two YC[3] :

a	$F^1_{2009} = 30468$, p<0.001
b	$F^1_{2009} = 1838$, p<0.001
c	$F^1_{2009} = 524$, p<0.001
t_{mat}	$F^1_{2009} = 256$, p<0.001

Difference in traits covariance between the two YC[4] : $\chi^2_{10} = 57$, p<0.001

[1] : likelihood ratio test comparing the fit of a model with a diagonal covariance matrix for the random effects and a model with no random effects (separately for each YC).

[2] : likelihood ratio test comparing the fit of a model with a symmetric co-variance matrix for the random effects and a model with a diagonal co-variance matrix (separately for each YC)

[3] : F tests of the YC effect coded as a factor acting linearly on the fixed part of parameters $\boldsymbol{\mu} \sim \boldsymbol{\mu}_0 + \boldsymbol{\mu}_1 \cdot YC$ in a model fitted on the two YC data pooled.

[4] : likelihood ratio test comparing the fit of a model on the two YC data pooled with a) a different random-effect co-variance matrix for each YC, and b) a similar co-variance matrix for the two YC.

644 **Table 3**. Estimates of the life history parameters and their correlation matrix for two year-
645 classes of NSSH (F.E.: fixed effects, sd(R.E): standard deviation of random effects). Units are
646 yr for t_{mat}, yr^{-1} for *b* and *c* and $kg^{1/4}.yr^{-1}$ for *a*.

647
648

	Norwegian spring spawning herring					
	YC 1933			**YC 1960**		
N	142			261		
Parameter mean and standard deviation estimates						
	F.E	sd(R.E)		F.E	sd(R.E)	
a	0.50	0.15		0.51	0.08	
b	0.42	0.18		0.28	0.08	
c	0.20	0.07		0.32	0.07	
t_{mat}	6.32	1.19		5.51	0.60	
Parameter correlation estimates						
	a	*b*	*c*	*a*	*b*	*c*
b	0.87			0.73		
c	0.13	-0.36		0.76	0.13	
t_{mat}	-0.34	0.15	-0.94	-0.96	-0.58	-0.84

649
650

651 **Table 4 :** Agreement between the growth based ($\hat{T}_{mat,i}$) and scales based ($T_{mat,i}$) estimates of

652 age at first reproduction for NSSH.

	Year-class 1933			Year-class 1960		
Age	n	Correct	Deviation ≤ 1	n	Correct	Deviation ≤ 1
4	1	100%	100%			
5	13	46%	100%	122	30%	100%
6	33	67%	97%	104	61%	97%
4	49	55%	92%	35	54%	97%
8	45	67%	93%			
9	1	100%	100%			
All ages	142	61%	94%	261	46%	98%

653
654
655

Figure legends

Fig. 1 : Growth curves for varying relative reproductive investment q ($q = c / (b+c)$, where b and c are size-specific maintenance and reproductive rates respectively) with fixed age at maturation, t_{mat} = 6 years, and fixed adult asymptotic size, $m_{\infty A}$=0.423 kg

Fig. 2 : Bias in the estimation of mean **a.** size-specific energy acquisition ($\hat{\bar{a}}$), **b-d.** maintenance ($\hat{\bar{b}}$) and reproductive investment ($\hat{\bar{c}}$) rates, and **e.** mean age at maturation ($\hat{\bar{t}}_{mat}$), from simulated growth data in relation to the true values of mean relative reproductive investment $\bar{q}$ and mean age at maturation $\bar{t}_{mat}$ used in the data simulation. Bias is expressed as the relative error $E_{\bar{x}}$ between the estimated and the true mean of each parameter (see Material and Methods section). White and black disks represent negative and positive bias respectively; size of the symbols indicates scale

Fig. 3 : Bias in the estimation of standard deviations for **a.** size-specific energy acquisition (σ_a), **c.** maintenance (σ_b) and **f.** reproductive investment (σ_c) rates, and **j.** age at maturation ($\sigma_{t_{mat}}$) and **b.,d.,e.,g.,h.,i.** correlations between these traits (ρ) from simulated growth data in relation to the true values of mean relative reproductive investment $\bar{q}$ and mean age at maturation $\bar{t}_{mat}$ used in the data simulation. Bias on standard deviation is expressed as the relative error E_{σ_x} (see Material and Methods section); bias on the correlations is expressed as the absolute difference between the estimated and true value

679 Fig. 4 : Error in the estimation of the individual size-specific **a.** energy acquisition ($\hat{a}_i$), **b.-d.**
680 maintenance ($\hat{b}_i$) and reproductive investment ($\hat{c}_i$) rates and **e.** age at maturation ($\hat{t}_{\mathrm{mat},i}$)
681 from simulated growth data in relation to the true values of mean relative reproductive
682 investment $\bar{q}$ and mean age at maturation $\bar{t}_{\mathrm{mat}}$ used in the data simulation. Error is
683 expressed as the mean of the absolute values of individual relative errors E_x (see
684 Material and Methods section)
685
686 Fig. 5 : Maturity ogives calculated from gonad observations in catch samples (triangles) and
687 from individual age at maturation estimated from back-calculated growth curves
688 (circles) with the corresponding fitted logistic models (dashed and solid lines
689 respectively) for the 1963 (filled symbols) and 1969 (empty symbols) year-classes of
690 North Sea plaice
691

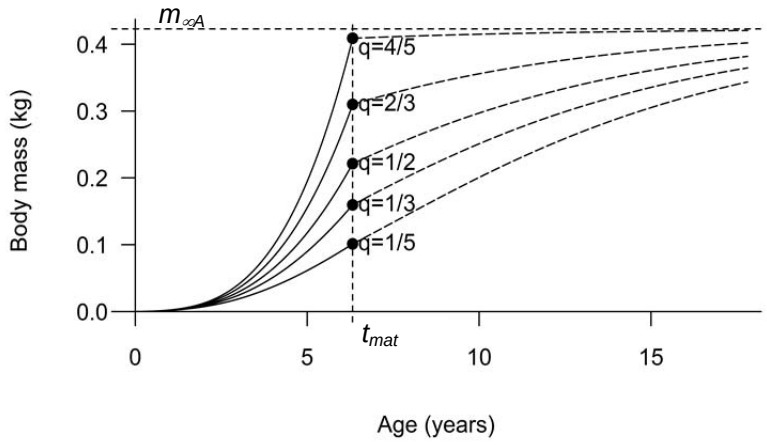

Fig. 1 Brunel et al.

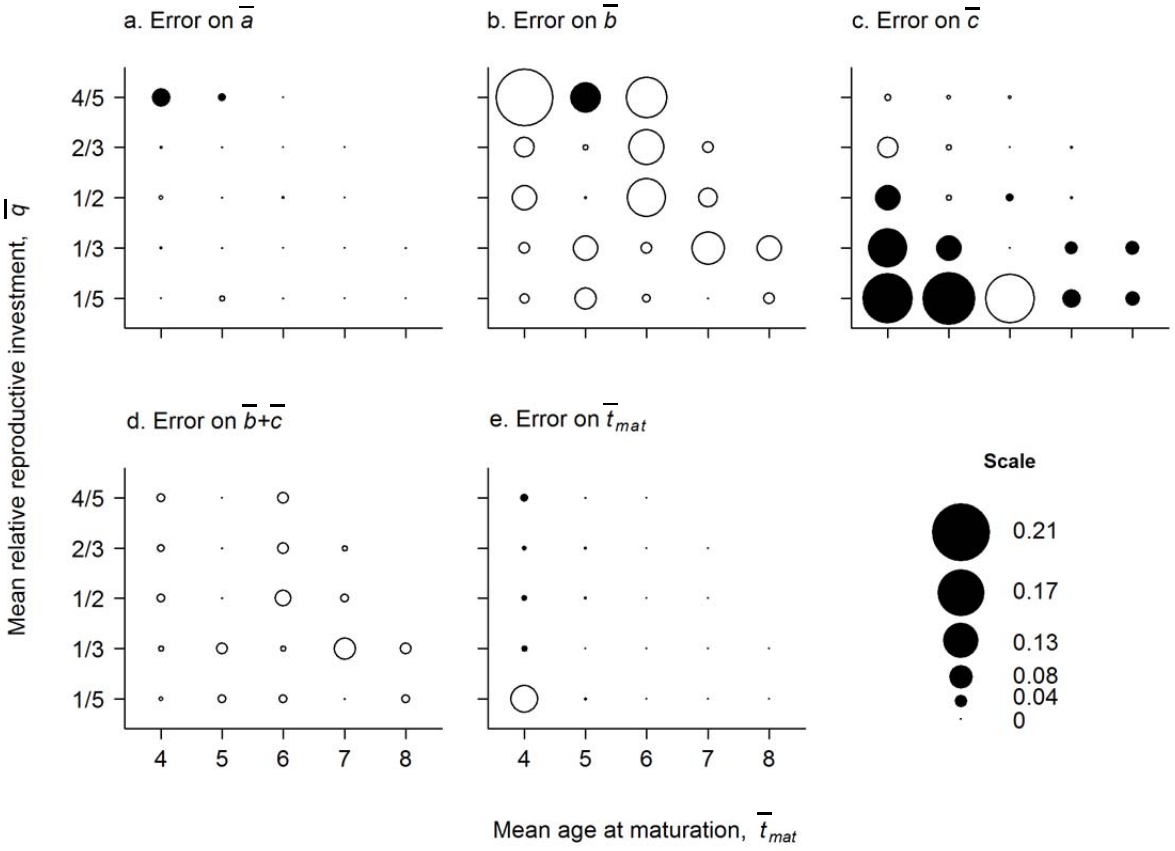

Fig. 2. Brunel et al.

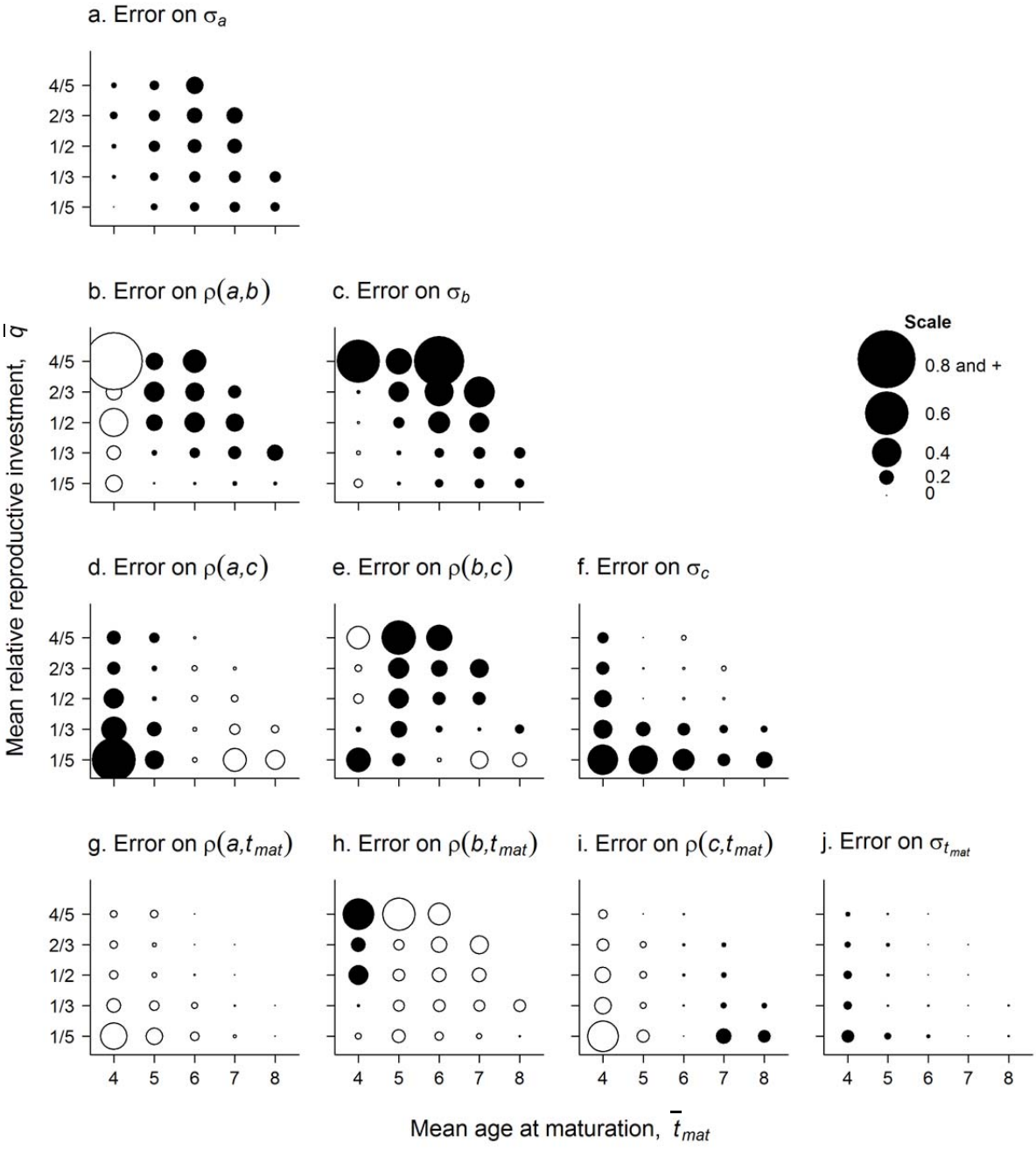

Fig. 3. Brunel et al.

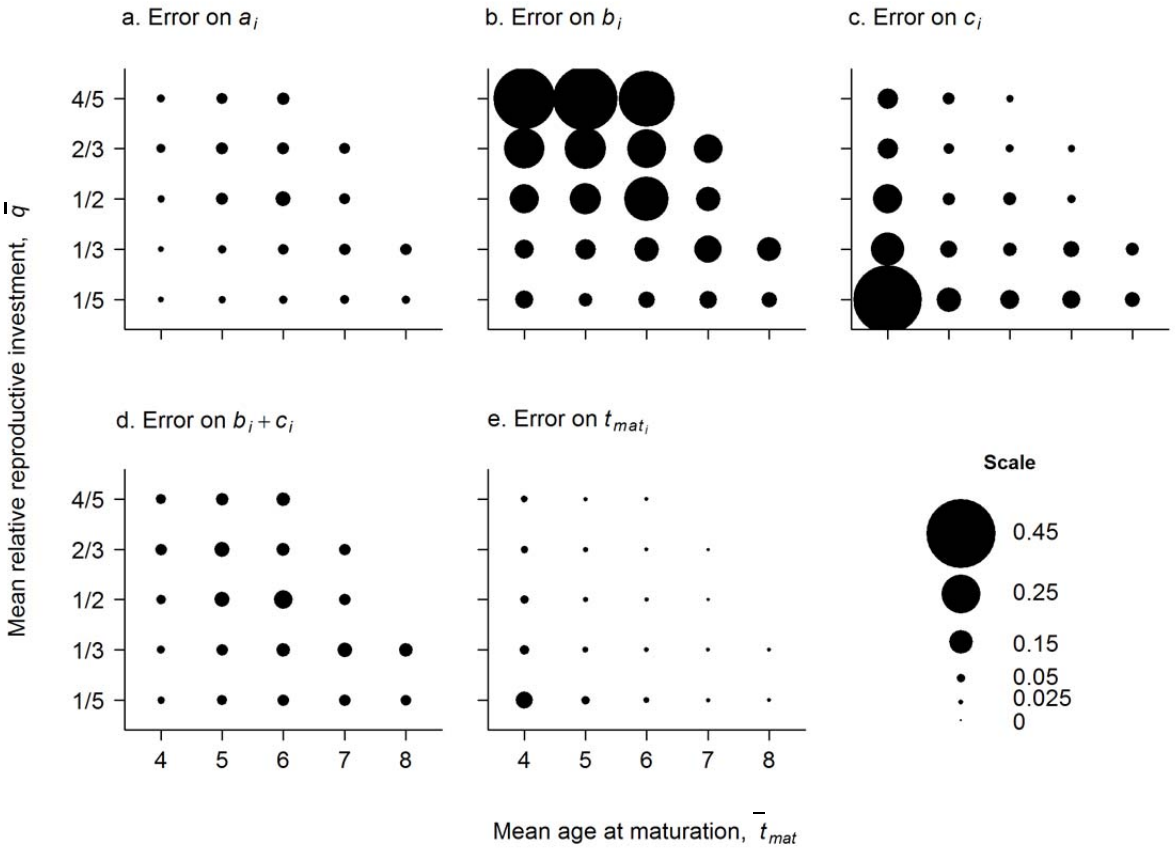

Fig. 4. Brunel et al.

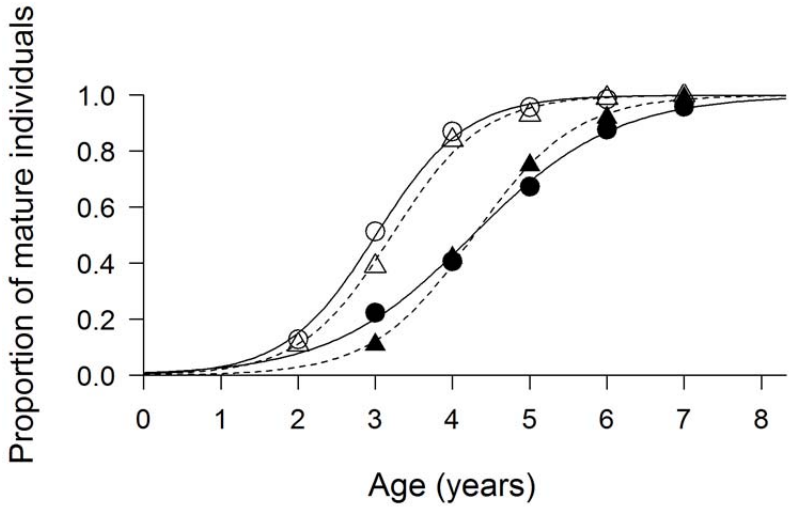

Fig. 5. Brunel et al.

Supplementary material for

Estimating age at maturation and energy-based life–history traits from individual growth trajectories with nonlinear mixed-effects models

by

Thomas Brunel, Bruno Ernande, Fabian Mollet and Adriaan D. Rijnsdorp

Supplementary material S 1:

Energy allocation-based growth model

Among all classes of energy allocation-based growth models, a frequently used differential equation for somatic growth, known as the Pütter balance equation (Pütter (1920) as cited in Ricklefs (2003)), has the following general form:

$$dm/dt = am^{\alpha} - bm^{\beta} \qquad \text{for } t \le t_{mat} \tag{S1a}$$

$$dm/dt = am^{\alpha} - bm^{\beta} - cm^{\gamma} \qquad \text{for } t > t_{mat} \tag{S1b}$$

where m is body mass, t is time, t_{mat} is age at maturation and the coefficients a, b and c are the size-specific rates of energy acquisition, energy use for body maintenance, and energy use for reproduction, respectively. According to this model, the amount of energy assimilated is used simultaneously for body maintenance, somatic growth and, after maturation, reproduction (figure S1). The relative importance of energy flows to maintenance, somatic growth and reproduction varies during the individual's lifetime, as *m* increases, depending on the value of exponents α, β and γ.

Several versions of this equation differing in these exponents values have been proposed in the literature (see e.g. Table 2 in Ricklefs (2003)). Among the most popular ones are those proposed by Von Bertalanffy ($\alpha = 2/3$ and $\beta = \gamma = 1$) (von Bertalanffy 1957) and West et al. ($\alpha = 3/4$ and $\beta = \gamma = 1$) (West et al. 2001). In von Bertalanffy's equation, the rate of energy acquisition is proportional to body surface which scales with $m^{2/3}$, whereas in West et al.'s model, the rate of energy acquisition is assumed to be limited by the size of the capillary network that brings energy to cells, which has a fractal form and scales with $m^{3/4}$. In our study, for the purpose of illustration we use the exponent values from West et al. because it has been intensively used in recent life history studies (Charnov et al. 2001; Economo et al. 2005).

The value of the scaling exponents of metabolic rates with body mass has been subject to considerable debates on both conceptual and empirical grounds (Allen and Gillooly 2007; O'Connor et al. 2007; Ricklefs 2003), the scaling power α of energy acquisition rate being the main point of controversy. However, using α=2/3 or α=3/4 results in very similar growth curves and performances in terms of goodness of fit (Banavar et al. 2002) and the results of

our study are almost unchanged whatever the exponent values chosen among these options. For NSP for instance, fitting the 1963 cohort data with $\alpha = 2/3$ gave similar estimates of age at maturation than the one presented in table 1, and, although they were of course rescaled, the estimates of size-specific energy rates correlated very well with those obtained with $\alpha = 3/4$ (results not shown).

In practice, as soon as maintenance and reproductive energy rates scale with a greater power of body mass than energy acquisition rate, i.e. $\beta > \alpha$ and $\gamma > \alpha$ (eq. (S1b)), the results of our study are almost unchanged whatever the actual exponent values. An *ad hoc* alternative to conceptual exponent values would consist in estimating empirically exponent values for each dataset considered. Among 26 fish species, empirical estimates of α range from 0.66 to 0.80 with mean 0.69 (Hanson et al. 1999), lying thus in between the most popular conceptual values: $\alpha = 2/3$ (von Bertalanffy 1957) and $\alpha = 3/4$ (West et al. 2001). For NSSH, no estimate was available in the literature, but for NSP, Fonds et al. (1992) found $\alpha = 0.78$, which is close to the value we used $\alpha = 3/4$.

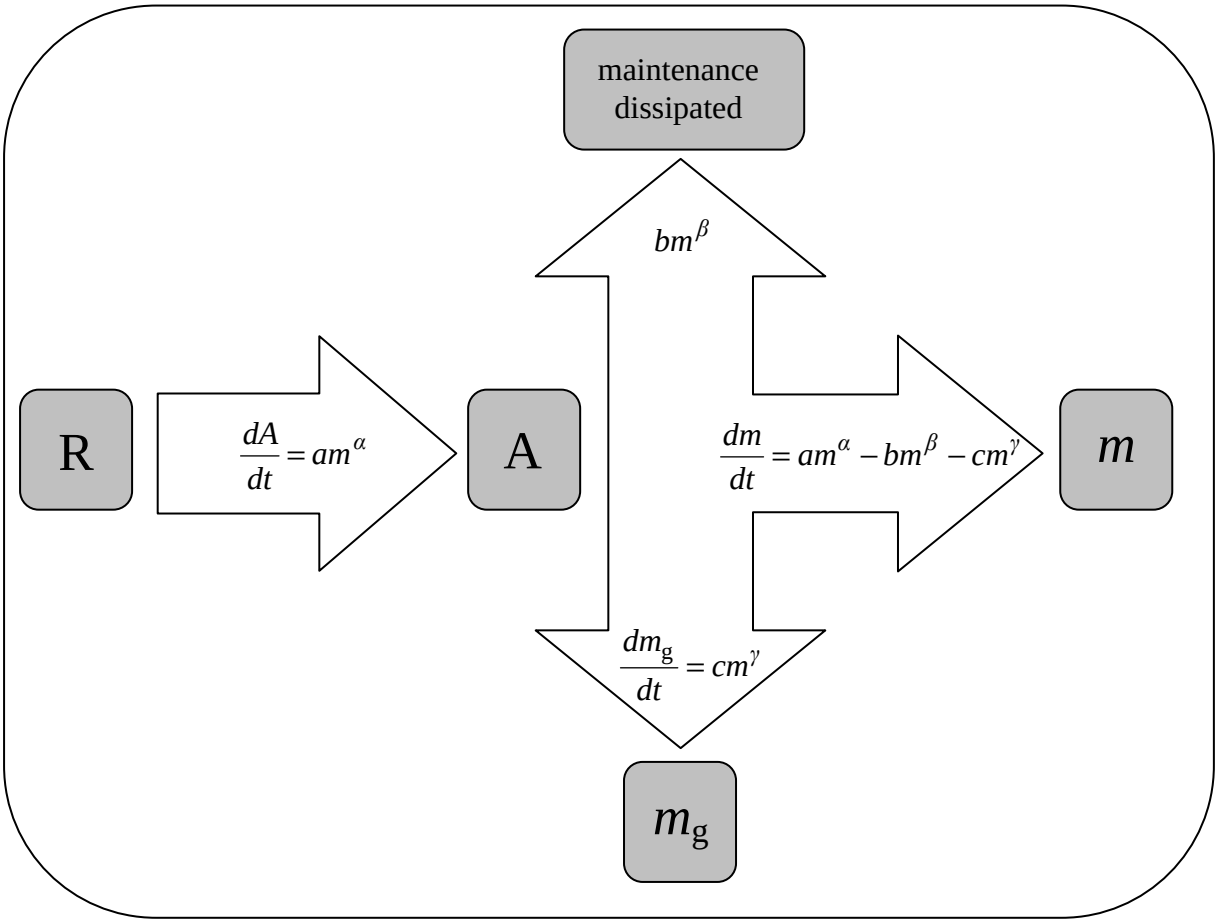

Figure S1 : Diagram of energy allocation in an adult individual according to Pütter balance equations, with R being resources in mass equivalent, A total acquired energy in mass equivalent, m_g gonad mass and m somatic mass. The rates of energy acquisition and

energy use by the three compartments (somatic mass, maintenance and gonad mass) are given by the equations in each arrows.

References

Allen AP, Gillooly JF (2007) The mechanistic basis of the metabolic theory of ecology. Oikos 116:1073-1077

Banavar JR, Damuth J, Maritan A, Rinaldo A (2002) Modelling universality and scaling. Nature 420:626

Charnov EL, Turner JH, Winemiller KO (2001) Reproductive constraints and the evolution of life histories with indeterminate growth. Proc. Natl. Acad. Sci. USA 98:9460-9464

Economo EP, Kerkhoff AJ, Enquist BJ (2005) Allometric growth, life-history invariants and population energetics. Ecol. Lett. 8:353-360

Fonds M, Cronie R, Vethaak AD, Van Der Puyl P (1992) Metabolism, food consumption and growth of plaice (*Pleuronectes platessa*) and flounder (*Platichthys flesus*) in relation to fish size and temperature. Neth J Sea Res 29:127-143

Hanson PC, Johnson TB, Schindler DE, Kitchell DE (1999) Fish bioenergetics 3.0. University of Wisconsin Seagrant Institute, Madison, WI

O'Connor MP et al. (2007) Reconsidering the mechanistic basis of the metabolic theory of ecology. Oikos 116:1058-1072

Pütter A (1920) Studien über Physiologische Ähnlichkeit. VI. Wachstumsähnlichkeiten. Pflügers Archive für Gesamte Physiologie Menschen und Tiere 180:298-340

Ricklefs RE (2003) Is rate of ontogenetic growth constrained by resource supply or tissue growth potential? A comment on West et *al.'s* model? Funct. Ecol 17:384-393

von Bertalanffy L (1957) Quantitative laws in metabolism and growth. Q. Rev. Biol 32:217-231

West GB, Brown JH, Enquist BJ (2001) A general model for ontogenetic growth. Nature 413:628-631

Supplementary material S 2:
Fitting the growth model using nonlinear mixed effect modelling

NLME models are commonly used for the analysis of longitudinal data (repeated measures over time on the same individuals), and to perform individual fits of a nonlinear parametric function for a set of individuals at once. In the present case, the formulation of the NLME model is the following one, with bold denoting vector and matrices:

$$m_{i,t} = m(t, \boldsymbol{\phi}_i) + \varepsilon_{i,t} \quad (4)$$

where $m_{i,t}$ is the body mass of the i^{th} individual at age t, $m(t, \boldsymbol{\phi}_i)$ is the growth model given by equation (3) with $\boldsymbol{\phi}_i = (a_i, b_i, c_i, t_{\text{mat},i})^{\text{T}}$ the vector of parameters to be estimated for the i^{th} individual, and $\varepsilon_{i,t}$ is a normally distributed error term.

NLME models estimate the vector of parameters $\boldsymbol{\phi}_i$ for each individual i as the sum of a vector of fixed effects $\boldsymbol{\mu} = (\bar{a}, \bar{b}, \bar{c}, \bar{t}_{\text{mat}})^{\text{T}}$ – the population means of the parameters – and a vector of random effects $\boldsymbol{\eta}_i = (\Delta a_i, \Delta b_i, \Delta c_i, \Delta t_{\text{mat},i})$ – the deviations of individual parameters from their population means:

$$\boldsymbol{\phi}_i = \boldsymbol{\mu} + \boldsymbol{\eta}_{\text{i}} \text{ where } \boldsymbol{\eta}_{\text{i}} \sim \text{MVN}(\mathbf{0}, \boldsymbol{\Sigma}^2), \quad (5)$$

where MVN refers to multivariate normal distribution. The random effects are constrained to follow a multivariate normal distribution $\text{MVN}(\mathbf{0}, \boldsymbol{\Sigma}^2)$ centered on $\mathbf{0}$, since they describe deviation from population means, with a variance-covariance matrix $\boldsymbol{\Sigma}^2$. In other terms, parameters of each individual growth curve are estimated given the 'average' population growth curve and assuming they are normally distributed in the population.

NLME models were fitted using the nlme package (Pinheiro et al. 2007) of the statistical software R (R Development Core Team 2006). Current algorithms have poor convergence properties when estimating more than 4 parameters. Therefore, we limited the number of estimated parameters to 4. To this end, for both the simulated and real datasets, the growth model was lagged by one year by replacing m_0 by m_1 and t by $t-1$ in equation (2) and m_1 was set constant at its mean value in the data.

The algorithm estimates the fixed effect parameters $\boldsymbol{\mu}$ using an iterative procedure that minimizes penalized nonlinear least squares, which requires providing starting values. The nonlinear least-square estimates of $\bar{a}$, $\bar{b}$, $\bar{c}$ and $\bar{t}_{\text{mat}}$ obtained by fitting the energy allocation model to the whole dataset considered (nls function, R base statistical software) were then used as starting values. As the confidence intervals produced by the nlme package are based on an approximation of the variance-covariance matrix of the parameter estimates obtained from the likelihood function, they are regarded as uncertain, and bootstrapping is considered more appropriate (Pinheiro and Bates, 2000). As bootstrapping (1000 replicates) combined to

fitting NLME is computationally very intensive, confidence intervals were produced only for NSP. For further details on NLME models and the fitting procedure used, the reader can refer to (Lindstrom and Bates 1990).

The NLME framework allows us to perform statistical tests on population level characteristics (parameters' means and (co-)variances),. Hypothesis tests are based on F tests for fixed effects and likelihood ratio tests between nested models that asymptotically follow a χ^2 under the null hypothesis for random effects' (co-)variances (Pinheiro and Bates 2000).

Lindstrom MJ, Bates DM (1990) Nonlinear Mixed Effects Models for Repeated Measures Data. Biometrics 46:673-687

Pinheiro J, Bates D, DebRoy S, Sarkar D, the R Core team (2007) nlme: Linear and Nonlinear Mixed Effects Models. R package version 3.1-86

R Development Core Team (2006) R: A language and environment for statistical computing. R Foundation for Statistical Computing, Vienna, Austria